Title	Nonlinear programming approach to form-finding and folding analysis of tensegrity structures using fictitious material properties
Author(s)	Ohsaki, M; Zhang, J.Y.
Citation	International Journal of Solids and Structures (2015), 69-70: 1-10
Issue Date	2015-09
URL	http://hdl.handle.net/2433/217067
Right	© 2015. This manuscript version is made available under the CC-BY-NC-ND 4.0 license http://creativecommons.org/licenses/by-nc-nd/4.0/ The full-text file will be made open to the public on 01 September 2017 in accordance with publisher's 'Terms and Conditions for Self-Archiving'.; The full-text file will be made open to the public on 01 September 2017 in accordance with publisher's 'Terms and Conditions for Self-Archiving'.; This is not the published version. Please cite only the published version. この論文は出版社版でありません。引用の際には出版社版をご確認ご利用ください。
Type	Journal Article
Textversion	author

Submitted to Int. J. Solids and Structures

Nonlinear Programming Approach to Form-finding and Folding Analysis of Tensegrity Structures using Fictitious Material Properties

***M. Ohsaki[1] and J.Y. Zhang[2]**

[1]Department of Architecture, Hiroshima University, Kagamiyama 1-4-1,
Higashi-Hiroshima 739-8527, Japan.
Currently, Department of Architecture and Architectural Engineering, Kyoto University,
Kyoto-daigaku Katsura, Nishikyo, Kyoto 615-8540, Japan
[2]Department of Architecture and Urban Design, Nagoya City University, Japan

*Corresponding author: ohsaki@archi.kyoto-u.ac.jp

Abstract

An optimization approach is presented for form-finding of tensegrity structures. It is shown that various equilibrium shapes can be easily found by solving a forced-deformation analysis problem formulated as a minimization problem considering the nodal coordinates as design variables. The objective function is defined in terms of the member lengths, and it can be regarded as the total strain energy corresponding to fictitious elastic material properties. The self-equilibrium forces can be found from the optimality conditions of the nonlinear programming problem. Stability of the self-equilibrium shape is investigated based on the local convexity of the objective function. Similarity between form-finding problem of a structure with zero-unstressed-length cables and the problem of minimum square-length network is also discussed. Furthermore, folding of a structure with small unstressed-length cables is approximately simulated using affine transformation of equilibrium shape.

Keywords: Tensegrity, Form-finding, Optimization, Stability, Affine transformation, Folding analysis

1. Introduction

Tensegrity structures consist of cables and struts that carry tensile and compressive forces, respectively. Although the history and definition of tensegrity structures are subject to

controversy (Hanaor, 2012), the structure considered here has discontinuous struts and no support. In a broader definition of tensegrity, the struts may contact with each other; however, prestress is always needed for ensuring enough stiffness against external loads. The weight of a tensegrity structure can be neglected if the prestress is large enough compared with the self-weight; accordingly, the member forces due to prestress constitute a self-equilibrium state without external load.

It is difficult to obtain a desired shape of a tensegrity structure, because the structure is generally kinematically indeterminate; i.e., it is unstable in absence of prestress, and the shape of the structure defined by nodal coordinates at a self-equilibrium state depends on the distribution of prestress. To overcome these difficulties, various analytical and numerical approaches have been developed for form-finding of tensegrity structures (Motro, 2003; Zhang and Ohsaki, 2006; Skelton and de Oliveira, 2009). Form-finding algorithms can be classified into kinematical method and statical method (Tibert and Pellegrino, 2003). The kinematical method minimizes the total cable length or the sum of squares of cable lengths with fixed total length of struts; alternatively, it maximizes the total strut length or the sum of squares of strut lengths with fixed total length of cables. The statical method directly solves the equilibrium equations.

In the kinematical method, optimization approaches are effectively used for minimizing/maximizing the functions of cable/strut lengths. Pagitz and Tur (2009) presented a two-stage algorithm based on minimization of the total potential energy by adjusting the cable lengths. Masic et al. (2005) presented a method for minimizing the quadratic error norm of the nodal locations from the target locations. They also formulated the problem of minimizing the error of the equilibrium equations. Miki and Kawaguchi (2010) proposed an approach to form-finding of cable networks and tensegrity structures by solving optimization problems with various objective functions and constraints. Gasparini et al. (2011) carried out form-finding using nonlinear programming (NLP) approach. They also discussed form-finding with constant stress elements as well as similarity between the penalty function approach and the constrained optimization approach. Chen et al. (2012) used an ant-colony optimization method. Li et al. (2010) solved a minimization problem of the total potential energy using a Mote Carlo method. Ohsaki et al. (2005) presented a method by minimizing the error of member forces from the target values. Burkhardt (2006) minimized the difference between squared sums of lengths of cables and struts. Zhang and Ohsaki (2007b) proposed a multiobjective programming approach considering the lowest positive eigenvalue of the tangent stiffness matrix and the compliance against specified loads, where convexity

properties of the objective functions are fully utilized to validate enumeration of the vertices of feasible region. The method has been extended to a hybrid optimization-antioptimization problem incorporating the errors of the member forces (Ohsaki et al., 2012). Ehara and Kanno (2010) developed a mixed-integer programming approach to topology design of a tensegrity structure consisting of discontinuous struts.

In the process of form-finding of a tensegrity structure that is free-standing, rigid-body motions should be appropriately constrained. Zhang et al. (2014) proposed an approach based on random selection of the six displacement components to be constrained. Zhang and Ohsaki (2013) proposed a method utilizing singular value decomposition or a generalized inverse of the tangent stiffness matrix. By contrast, for a cable net that has fixed supports, the equilibrium shape can be found by simply minimizing the total strain energy, which is a convex function of the nodal coordinates, under convex constraints (Kanno et al. 2002).

It is well known that fictitious material properties with various stress-strain relations can be used for form-finding for specified forces (Pagitz and Tur, 2009; Miki et al., 2013). Fictitious damping is also widely used for the dynamic relaxation method for form-finding. Schenk et al. (2007) investigated the stiffness of a tensegrity structure with zero-unstressed-length cables, and showed that such structure has zero-stiffness if the directional vectors of struts lie on a projective conic, which means that the strut lengths do not change due to deformation; accordingly, no external force is needed in the process of an affine transformation or a similarity transformation (Masic et al., 2005, Zhang and Ohsaki, 2007a).

For folding and deployment of a tensegrity structure, it is preferable to utilize a flexible/compliant mechanism with self-equilibrium forces (Ohsaki and Nishiwaki, 2005; Ohsaki et al., 2013), because such a structure is stable without additional restraint (Smaili and Motro, 2005, 2007). Deployment of folded tensegrity structures is very important for application to space structures. Infinitesimal mechanism can also be utilized for reducing energy required for folding (Sultan, 2014). Arsenault and Gosselin (2005, 2006) analytically investigated kinematic properties of tensegrity mechanisms. The folding process can be simulated by tracking the path of equilibrium state called equilibrium manifold (Micheletti and Williams, 2007; Sultan and Skelton, 2003). Deployment of ring modules is studied by Rhode-Barbarigos et al. (2012).

In view of practical application of form-finding of a tensegrity structure, it is very important to ensure stability of the equilibrium state, because an unstable solution cannot be actually manufactured. Guest (2006) investigated stiffness of prestressed framework, and presented a simple approach to derivation of tangent stiffness matrix. Ohsaki and Zhang

(2006) and Zhang and Ohsaki (2007a) investigated the conditions for stability, prestress-stability, and super-stability of tensegrity structures. Deng and Kwan (2005) presented an energy-based approach to classification of stability of pin-jointed frameworks.

In this paper, we present a method for form-finding of tensegrity structures using a nonlinear programming (NLP) approach. Various equilibrium shapes are found by solving a forced-deformation analysis problem formulated as a minimization problem of a function of the nodal coordinates in terms of member lengths. The problem is regarded as a minimization problem of the total strain energy with fictitious elastic material properties. The self-equilibrium forces can be found from the optimality conditions of the NLP problem. We apply the method to tensegrity towers with bilinear elastic stress-strain relation for some selected cables. Stability is guaranteed, except for the fictitious material with softening property, from the local convexity of the objective function; hence, stiffness matrices are not needed for investigation of stability. Similarity between form-finding problem of zero-unstressed-length cables and the problem of minimum square-length network is also discussed. It is shown that a tensegrity structure can be folded with small external forces, if the unstressed lengths of cables are small. However, the convergence property of the optimization problem is deteriorated if the unstressed lengths of cables are very small. To resolve this difficulty, we present a simple form for invariance property of the equilibrium equations with respect to affine transformation, and approximately simulate the folding of a structure with small unstressed-length cables using the affine transformation of equilibrium shape. The proposed method is applied to folding analysis of a tensegrity tower, and it is confirmed that the force density matrix remains unchanged and the required force is very small if cables with small unstressed lengths are used.

2. Basic properties and equations

Consider a tensegrity structure consisting of cables and struts. Although the definition of a tensegrity structure is controversial, the structure considered in this paper is clearly defined as follows:

1. Cables and struts transmit only tensile and compressive forces, respectively.
2. The structure has no support; i.e., it is free-standing with three translational and three rotational rigid-body motions.
3. Cables and struts are pin-jointed; therefore, the structure can be modeled using truss elements, and no friction or sliding occurs at the joints.

4. The level of prestress is large enough compared with the self-weight of structure; therefore, the self-weight is neglected, and there is no external nodal load at the self-equilibrium state.

We define the basic vectors and matrices below, for completeness of the paper. See, e.g., Zhang and Ohsaki (2006, 2015), for details.

Let n and m denote the numbers of nodes and members, respectively. The topology of a tensegrity structure is defined using the connectivity (incidence) matrix $\mathbf{C} \in \mathbb{R}^{m \times n}$. If nodes i and j $(i < j)$ are connected by member k, then the i th and j th elements in the k th row of $\mathbf{C}$ are equal to 1 and -1, respectively, while all other elements in the k th row are 0 (Skelton and de Oliveira, 2009; Zhang and Ohsaki, 2015).

The coordinates of the i th node at a self-equilibrium state is denoted by (x_i, y_i, z_i). The vectors of x-, y-, z-coordinates are given as $\mathbf{x}$, $\mathbf{y}$, $\mathbf{z}$ $(\in \mathbb{R}^n)$, and the vector of all nodal coordinates is defined as $\mathbf{X} = (\mathbf{x}^T, \mathbf{y}^T, \mathbf{z}^T)^T \in \mathbb{R}^{3n}$. The length and axial force of the i th member at the self-equilibrium state is denoted by L_i and N_i, respectively. Let $q_i = N_i / L_i$ denote the force density of member i, and define the force density vector as $\mathbf{q} = (q_1, \ldots, q_m)^T$. Then, the force density matrix $\mathbf{Q} \in \mathbb{R}^{n \times n}$ is given as

$$\mathbf{Q} = \mathbf{C}^T \operatorname{diag}(\mathbf{q}) \mathbf{C} \tag{1}$$

Alternatively, the (i, j)-component $Q_{i,j}$ of $\mathbf{Q}$ is explicitly given as

$$Q_{i,j} = \begin{cases} \sum_{k \in I} q_k, & \text{if} \quad i = j \\ -q_k, & \text{if nodes } i \text{ and } j \text{ are connected by member } k \\ 0, & \text{otherwise} \end{cases} \tag{2}$$

where I is the set of members connected to node i.

The self-equilibrium equation with respect to the nodal coordinates can be written using $\mathbf{Q}$ as

$$\mathbf{Q}\mathbf{x} = \mathbf{0}, \quad \mathbf{Q}\mathbf{y} = \mathbf{0}, \quad \mathbf{Q}\mathbf{z} = \mathbf{0} \tag{3}$$

The coordinate difference matrices $\mathbf{U}^x$, $\mathbf{U}^y$, and $\mathbf{U}^z$ $(\in \mathbb{R}^{m \times m})$ in x-, y-, and z-directions, respectively, of members are defined as

$$\mathbf{U}^x = \operatorname{diag}(\mathbf{C}\mathbf{x}), \quad \mathbf{U}^y = \operatorname{diag}(\mathbf{C}\mathbf{y}), \quad \mathbf{U}^z = \operatorname{diag}(\mathbf{C}\mathbf{z}) \tag{4}$$

The i th diagonal components of $\mathbf{U}^x$, $\mathbf{U}^y$, and $\mathbf{U}^z$ are denoted by U_i^x, U_i^y, and U_i^z,

respectively. The directional cosines θ_i^x, θ_i^x, and θ_i^x of member i with respect to x-, y-, and z-axes, respectively, are obtained as

$$\theta_i^x = \frac{U_i^x}{L_i}, \quad \theta_i^y = \frac{U_i^y}{L_i}, \quad \theta_i^z = \frac{U_i^z}{L_i} \tag{5}$$

and their matrix forms $\mathbf{\Theta}^x$, $\mathbf{\Theta}^y$, and $\mathbf{\Theta}^z$ $(\in \mathbb{R}^{m\times m})$ are given as

$$\mathbf{\Theta}^x = \mathrm{diag}(\theta_1^x,\ldots,\theta_m^x), \quad \mathbf{\Theta}^y = \mathrm{diag}(\theta_1^y,\ldots,\theta_m^y), \quad \mathbf{\Theta}^z = \mathrm{diag}(\theta_1^z,\ldots,\theta_m^z) \tag{6}$$

Then, the equilibrium matrix $\mathbf{D}$ is written as

$$\mathbf{D} = \begin{pmatrix} \mathbf{C}^T\mathbf{\Theta}^x \\ \mathbf{C}^T\mathbf{\Theta}^y \\ \mathbf{C}^T\mathbf{\Theta}^z \end{pmatrix} \tag{7}$$

Since we neglect the self-weight, the self-equilibrium equation with respect to the member force vector $\mathbf{N} = (N_1,\ldots,N_m)^T$ is formulated as

$$\mathbf{DN} = \mathbf{0} \tag{8}$$

Suppose the unstressed lengths L_i^0 $(i = 1,\ldots,m)$ of members are given. The members are connected to satisfy the specified compatibility (connectivity) conditions at nodes. The member lengths $L_i(\mathbf{X})$ $(i = 1,\ldots,m)$ satisfying the compatibility conditions are found by solving a geometrically nonlinear analysis problem subjected to forced deformation; hence, $L_i(\mathbf{X})$ is regarded as a function of $\mathbf{X}$. The axial forces $N_i(\mathbf{X})$ $(i = 1,\ldots,m)$ are also found by solving the analysis problem. This way, the form-finding problem is formulated as a forced-deformation analysis problem with variable vector $\mathbf{X}$.

The square of member length is expressed in terms of coordinate differences as

$$L_i(\mathbf{X})^2 = U_i^x(\mathbf{X})^2 + U_i^y(\mathbf{X})^2 + U_i^z(\mathbf{X})^2 \tag{9}$$

Differentiation of Eq. (9) with respect to $\mathbf{X}$ leads to

$$\nabla L_i(\mathbf{X}) = \frac{U_i^x(\mathbf{X})}{L_i(\mathbf{X})}\nabla U_i^x(\mathbf{X}) + \frac{U_i^y(\mathbf{X})}{L_i(\mathbf{X})}\nabla U_i^y(\mathbf{X}) + \frac{U_i^z(\mathbf{X})}{L_i(\mathbf{X})}\nabla U_i^z(\mathbf{X}) \tag{10}$$

which can be written using the directional cosines as

$$\nabla L_i(\mathbf{X}) = \theta_i^x(\mathbf{X})\nabla U_i^x(\mathbf{X}) + \theta_i^y(\mathbf{X})\nabla U_i^y(\mathbf{X}) + \theta_i^z(\mathbf{X})\nabla U_i^z(\mathbf{X}) \tag{11}$$

From Eqs. (4) and (11), the following relation holds:

$$\sum_{i=1}^{m} N_i(\mathbf{X})\nabla L_i(\mathbf{X}) = \begin{pmatrix} \mathbf{C}^T\mathbf{\Theta}^x(\mathbf{X})\mathbf{N}(\mathbf{X}) \\ \mathbf{C}^T\mathbf{\Theta}^y(\mathbf{X})\mathbf{N}(\mathbf{X}) \\ \mathbf{C}^T\mathbf{\Theta}^z(\mathbf{X})\mathbf{N}(\mathbf{X}) \end{pmatrix} = \begin{pmatrix} \mathbf{C}^T\mathbf{\Theta}^x(\mathbf{X}) \\ \mathbf{C}^T\mathbf{\Theta}^y(\mathbf{X}) \\ \mathbf{C}^T\mathbf{\Theta}^z(\mathbf{X}) \end{pmatrix}\mathbf{N}(\mathbf{X}) \tag{12}$$

which is equivalent to Eq.(8). Hence, the self-equilibrium equation can be written as

$$\sum_{i=1}^{m} N_i(\mathbf{X})\nabla L_i(\mathbf{X}) = \mathbf{0} \tag{13}$$

3. Nonlinear programming approach to form finding using fictitious materials

3.1 Optimization problem and equilibrium conditions

We formulate the form-finding problem as a minimization problem of a function with respect to the nodal coordinates. Although the properties of a tensegrity structure are defined based on the materials of the cables and struts, we can use a fictitious material in the process of form-finding for generating nodal coordinates and axial forces of various self-equilibrium shapes. The structure is actually realized using the true material, and the unstressed lengths are found so that the nodal coordinates and axial forces do not change after assigning the true material properties. Folding of a tensegrity structure with small unstressed-length cables can also be simulated using a fictitious cable material that has zero-unstressed length.

A continuously differentiable function of $\mathbf{X}$ in terms of the member lengths $L_i(\mathbf{X})$ is defined as

$$F(\mathbf{X}) = \sum_{i=1}^{m} F_i(L_i(\mathbf{X})) \tag{14}$$

An unconstrained optimization problem is formulated as

$$\text{Minimize} \quad F(\mathbf{X}) = \sum_{i=1}^{m} F_i(L_i(\mathbf{X})) \tag{15}$$

Note that $\mathbf{X}$ should be in the feasible region satisfying the sign requirements of axial forces in cables and struts. The stationary condition of $F(\mathbf{X})$ is written as

$$\nabla F(\mathbf{X}) = \sum_{i=1}^{m} \frac{\partial F_i(L_i(\mathbf{X}))}{\partial L_i(\mathbf{X})} \nabla L_i(\mathbf{X}) = \mathbf{0} \tag{16}$$

If $F(\mathbf{X})$ is a locally convex function in the neighborhood of the solution $\mathbf{X} = \mathbf{X}^s$ satisfying Eq. (16), then $\mathbf{X}^s$ is a local optimal solution, and the hessian $\nabla^2 F(\mathbf{X})$ of $F(\mathbf{X})$ is positive definite at $\mathbf{X} = \mathbf{X}^s$.

We consider a fictitious material satisfying

$$N_i(\mathbf{X}) = \frac{\partial F_i(L_i(\mathbf{X}))}{\partial L_i(\mathbf{X})} \tag{17}$$

Then, Eq.(16) is equivalent to the equilibrium equation (13). This way, a self-equilibrium

shape can be found by minimizing a function of member lengths.

3.2 Stability of the self-equilibrium state

Although minimization of a function of member lengths is not new for form-finding of tensegrity structures, stability of the obtained self-equilibrium state has not been fully investigated. We present an approach to stability investigation without resort to stiffness matrices.

There are several definitions of stability used in the field of structural mechanics. The most common definition is the positive definiteness of the tangent stiffness matrix, which is derived from the definition of asymptotic stability based on Liapunov's direct method (La Salle and Lefscetz, 1961) assuming existence of appropriate damping.

If we can regard $F(\mathbf{X})$ as a Liapunov function, then the equilibrium state obtained by solving Problem (15) is stable, if $F(\mathbf{X})$ is a strictly quasi-convex function in the neighborhood of the equilibrium state and $\nabla F(\mathbf{X})$ corresponds to the restoring force of the structure (Ohsaki, 2003). On the other hand, the continuous function $F(\mathbf{X})$ is strictly quasi-convex in the neighborhood of a local minimum, if it is found by an NLP algorithm. Therefore, the equilibrium state found by minimizing $F(\mathbf{X})$ using the fictitious material is always stable. By contrast, if the objective function is not convex, then stability of the equilibrium state obtained by optimization is not guaranteed.

Further differentiation of $\nabla F(\mathbf{X})$ in Eq. (16) with respect to $\mathbf{X}$ leads to the Hessian of $F(\mathbf{X})$ as

$$\nabla^2 F(\mathbf{X}) = \sum_{i=1}^{m} \frac{\partial^2 F_i(L_i(\mathbf{X}))}{\partial^2 L_i(\mathbf{X})} \left[\nabla L_i(\mathbf{X}) \nabla^T L_i(\mathbf{X}) \right] + \sum_{i=1}^{m} \frac{\partial F_i(L_i(\mathbf{X}))}{\partial L_i(\mathbf{X})} \nabla^2 L_i(\mathbf{X}) \tag{18}$$

The Hessian $\nabla^2 F(\mathbf{X})$ is positive definite, when the optimization algorithm reaches an isolated local minimum of $F(\mathbf{X})$.

3.3 Minimization of strain energy using fictitious material

The total strain energy may be a natural choice for the objective function. For the given unstressed member length, the strain energy of member i is regarded as a function of $L_i(\mathbf{X})$, which is denoted by $S_i(L_i(\mathbf{X}))$.

Let A_i, E_i, and L_i^0 denote the cross-sectional area, Young's modulus and the unstressed length of member i. The strain energy of member i is defined as

$$S_i(L_i(\mathbf{X})) = \frac{E_i A_i}{2L_i^0}(L_i(\mathbf{X}) - L_i^0)^2 \tag{19}$$

Then, the total strain energy $S(\mathbf{X})$ is obtained as

$$S(\mathbf{X}) = \sum_{i=1}^{m} S_i(L_i(\mathbf{X})) \tag{20}$$

The self-equilibrium shape is found by solving an optimization problem of minimizing $S(\mathbf{X})$. When no constraint is given, the stationary condition of $S(\mathbf{X})$ is written as

$$\nabla S(\mathbf{X}) = \sum_{i=1}^{m} \frac{\partial S_i(L_i(\mathbf{X}))}{\partial L_i(\mathbf{X})} \nabla L_i(\mathbf{X}) = \mathbf{0} \tag{21}$$

At the optimal solution satisfying Eq. (21), the equilibrium equation (13) is satisfied, because $\partial S_i(L_i(\mathbf{X})) / \partial L_i(\mathbf{X})$ is the axial force $N_i(\mathbf{X})$ of member i as

$$N_i(\mathbf{X}) = \frac{\partial S_i(L_i(\mathbf{X}))}{\partial L_i(\mathbf{X})} = \frac{E_i A_i}{L_i^0}(L_i(\mathbf{X}) - L_i^0) \tag{22}$$

When the objective function is the total strain energy, the optimization problem to be solved for form-finding is a standard analysis problem with forced deformation to satisfy the compatibility at nodes for specified unstressed member lengths. Therefore, the principle of minimum total potential energy ensures stability of the equilibrium shape obtained by minimizing the strain energy of the structure without external loads.

Although the stiffness matrices are not necessary in the process of finding a stable self-equilibrium state, the tangent stiffness matrix is used in the numerical examples for confirmation of stability of the equilibrium state. By incorporating $S(\mathbf{X})$ into $F(\mathbf{X})$ in Eq. (18), the first and second terms in the right-hand side turns out to be the linear stiffness matrix $\mathbf{K}_{\mathrm{L}} \in \mathbb{R}^{3n\times 3n}$ and geometrical stiffness matrix $\mathbf{K}_{\mathrm{G}} \in \mathbb{R}^{3n\times 3n}$, respectively, which are given without derivation and omitting the variable $\mathbf{X}$ as

$$\mathbf{K}_{\mathrm{E}} = \mathbf{D}\bar{\mathbf{K}}\mathbf{D}^T, \quad \mathbf{K}_{\mathrm{G}} = \begin{pmatrix} \mathbf{Q} & & \\ & \mathbf{Q} & \\ & & \mathbf{Q} \end{pmatrix} \tag{23}$$

where

$$\bar{\mathbf{K}} = \mathrm{diag}(E_1 A_1 / L_1, \ldots, E_m A_m / L_m) \tag{24}$$

See, e.g., Zhang and Ohsaki (2007a) for details. Note that the member lengths at self-equilibrium state is usually used in Eq. (24). Then, the tangent stiffness matrix $\mathbf{K}_\mathrm{T} \in \mathbb{R}^{3n \times 3n}$ is given as

$$\mathbf{K}_\mathrm{T} = \mathbf{K}_\mathrm{E} + \mathbf{K}_\mathrm{G} \tag{25}$$

4. Fictitious materials of cables

Fictitious materials are used for cables in the process of form finding. The true material and a large cross-sectional area are used for struts so that they have sufficiently larger stiffness than cables.

4.1 Bilinear material

A bilinear elastic stress-strain relation is given for a cable as shown in Fig. 1. The materials in Cases 1 and 2 are linear elastic and stiffening bilinear, respectively. Case 3 has a softening bilinear property with a positive stiffness in the second part to ensure local minimum of $S(\mathbf{X})$ at the equilibrium state.

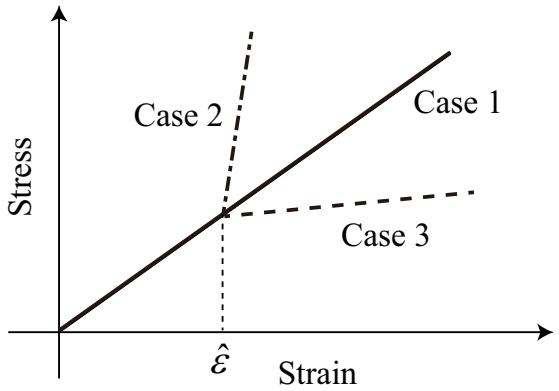

Figure 1. Linear and bilinear elastic stress-strain relations for cables.

The value of strain ε at the transition point of the bilinear elastic property is denoted by $\hat{\varepsilon}$; i.e., the length L_i^U at the transition point is $L_i^\mathrm{U} = (1+\hat{\varepsilon})L_i^0$. The elastic modulus for $L_i(\mathbf{X}) > L_i^\mathrm{U}$ of cable i is denoted by $\hat{E}_i$. Then, the strain energy for $L_i(\mathbf{X}) > L_i^\mathrm{U}$ of cable i is formulated as

$$S_i(L_i(\mathbf{X})) = \frac{E_i A_i}{2L_i^0}(L_j^\mathrm{U} - L_i^0)^2 + \frac{E_i A_i}{L_i^0} L_j^\mathrm{U}(L_i(\mathbf{X}) - L_j^\mathrm{U}) + \frac{\hat{E}_i A_i}{2L_i^0}(L_i(\mathbf{X}) - L_i^\mathrm{U})^2 \tag{26}$$

Differentiation of $S_i(L_i(\mathbf{X}))$ with respect to $\mathbf{X}$ leads to

$$\frac{\partial S_i(L_i(\mathbf{X}))}{\partial \mathbf{X}} = \frac{E_i A_i}{L_i^0} L_i^{\mathrm{U}} \nabla L_i(\mathbf{X}) + \frac{\hat{E}_i A_i}{L_i^0}(L_i(\mathbf{X}) - L_i^{\mathrm{U}}) \nabla L_i(\mathbf{X}) \tag{27}$$

From Eqs. (13) and (27), the axial force at equilibrium is obtained as follows at the solution $\mathbf{X}^{\mathrm{s}}$ that minimizes $S(\mathbf{X})$:

$$N_i(\mathbf{X}^{\mathrm{s}}) = \frac{E_i A_i}{L_i^0} L_i^{\mathrm{U}} + \frac{\hat{E}_i A_i}{L_i^0}(L_i(\mathbf{X}^{\mathrm{s}}) - L_i^{\mathrm{U}}) \tag{28}$$

Let $\tilde{A}_i$ and $\tilde{E}_i$ denote the cross-sectional area and Young's modulus of the true linear elastic material. The unstressed length $\tilde{L}_i^0$ of the cable with the true material is found to satisfy the following relation so that its axial force is equal to $N_i(\mathbf{X}^{\mathrm{s}})$:

$$\frac{\tilde{E}_i \tilde{A}_i}{\tilde{L}_i^0}(L_i(\mathbf{X}^{\mathrm{s}}) - \tilde{L}_i^0) = \frac{E_i A_i}{L_i^0} L_i^{\mathrm{U}} + \frac{\hat{E}_i A_i}{L_i^0}(L_i(\mathbf{X}^{\mathrm{s}}) - L_i^{\mathrm{U}}) \tag{29}$$

When an equilibrium state is found using an optimization algorithm, it corresponds to a local minimum of $S(\mathbf{X})$ using the fictitious material, which means $S(\mathbf{X})$ is locally convex at $\mathbf{X} = \mathbf{X}^{\mathrm{s}}$ and the equilibrium state is stable. The strain energy function using the true material is also convex, if the following relation is satisfied:

$$\frac{\tilde{E}_i \tilde{A}_i}{\tilde{L}_i^0} \geq \frac{\hat{E}_i A_i}{L_i^0} \tag{30}$$

In this case, the structure with true material is also stable. Note that the condition in Eq. (30) is a sufficient but not a necessary condition for stability.

Member numbers are assigned, for simplicity, such that members $1,\ldots,m_{\mathrm{c}}$ are cables and members $m_{\mathrm{c}}+1,\ldots,m$ are struts. For Case 2, we can formulate a constrained optimization problem with upper bound L_i^{U} for cable i as

$$\begin{aligned} &\text{Minimize} \quad S(\mathbf{X}) = \sum_{i=1}^{m} S_i(L_i(\mathbf{X})) \\ &\text{Subject to} \quad L_i(\mathbf{X}) - L_i^{\mathrm{U}} \leq 0, \quad (i = 1, \ldots, m_{\mathrm{c}}) \end{aligned} \tag{31}$$

Let λ_i denote the Lagrange multiplier for the i th constraint in Eq. (31). The optimality conditions (KKT conditions) for the constrained minimization problem (31) is written as

$$\sum_{i=1}^{m} \frac{\partial S_i(L_i(\mathbf{X}))}{\partial L_i(\mathbf{X})} \nabla L_i(\mathbf{X}) + \sum_{i=1}^{m_{\mathrm{c}}} \lambda_i \nabla L_i(\mathbf{X}) = \mathbf{0}$$

$$\lambda_i \geq 0\,, \quad \lambda_i(L_i(\mathbf{X}) - L_i^{\mathrm{U}}) = 0\,, \quad L_i(\mathbf{X}) - L_i^{\mathrm{U}} \leq 0\,, \quad (i = 1, \ldots, m_{\mathrm{c}}) \tag{32}$$

Hence, the equilibrium equation (13) is satisfied by regarding $N_i(\mathbf{X}) = \partial S_i(L_i(\mathbf{X})) / \partial L_i(\mathbf{X}) + \lambda_i$ for cables and $N_i(\mathbf{X}) = \partial S_i(L_i(\mathbf{X})) / \partial L_i(\mathbf{X})$ for struts.

A similar formulation is derived by Miki and Kawaguchi (2010); however, their purpose is to find an equilibrium shape by minimizing a function of cable lengths under constraints on the strut lengths. Note that the sufficient condition (30) for stability of the structure with true material is not ensured for Case 2. This is observed from the KKT condition (32) that additional tensile force corresponding to the Lagrange multiplier λ_i (> 0) should be applied to cable *i* to restrict the deformation of the cable.

4.2 Zero-unstressed-length cable

Schenk et al. (2007) investigated the properties of tensegrity structures, where each cable has zero unstressed length, and demonstrated that such cables can be manufactured using conventional springs attached alongside bars. A cable with small unstressed length can be modeled using a flexible spring or rubber. By assuming $L_i(\mathbf{X}) \gg L_i^0$ in Eq. (19), the strain energy of member i is formulated as

$$S_i^*(L_i(\mathbf{X})) = \frac{E_i A_i}{2L_i^0}(L_i(\mathbf{X}))^2 \tag{33}$$

Note that the coefficient $EA/(2L_i^0)$ diverges to infinity in the limit $L_i^0 \to 0$.

This formulation is closely related to form-finding analysis based on minimum square-length network that has the smallest total square length of cables for the given strut lengths. Since $E_i A_i / L_i^0$ is the extensional stiffness of the cable, we can rewrite Eq. (33) as follows using $k_i = E_i A_i / L_i^0$:

$$S_i^*(L_i(\mathbf{X})) = \frac{k_i}{2}(L_i(\mathbf{X}))^2 \tag{34}$$

From Eqs. (22) and (34), we obtain

$$N_i(\mathbf{X}) = \frac{\partial S_i^*(L_i(\mathbf{X}))}{\partial L_i(\mathbf{X})} = k_i L_i(\mathbf{X}) \tag{35}$$

Therefore, the force density q_i of a cable at the equilibrium state $\mathbf{X} = \mathbf{X}^{\mathrm{s}}$ should be equal to the specified stiffness as

$$q_i = \frac{N_i(\mathbf{X}^s)}{L_i(\mathbf{X}^s)} = k_i \tag{36}$$

Note that the matrix **Q** in Eq. (3), which is a linear function of the force density vector $\mathbf{q} = (q_1, \ldots, q_m)^T$ as in Eq. (1), should have four zero eigenvalues in order to realize an equilibrium shape in 3-dimensional space (Zhang and Ohsaki, 2006). It is easily observed from the definition in Eq. (2) that the vector $(1, \ldots, 1)^T$ is one of the eigenvector corresponding to a zero eigenvalue irrespective of the values of q_i. Therefore, **q** should satisfy three nonlinear equations to ensure a 3-dimensional tensegrity structure, which means that force densities of cables generally cannot have specified values as Eq. (36), and minimization of the sum of $S_i^*(L_i(\mathbf{X}))$ leads to a shape in a smaller dimension; i.e., plane, line, or point. This fact is consistent with the observation by Miki and Kawaguchi (2010) noting that minimizing the sum of $S_i^*(L_i(\mathbf{X}))$ does not easily lead to a stable 3-dimensional configuration.

By contrast, if the unstressed length is moderately large, and $S_i(L_i(\mathbf{X}))$ in Eq. (19) is used, a wide range of force densities can be covered, and there exists more possibility of generating a shape in 3-dimensional space. Figure 2 shows variation of $q_i = k_i(L_i - L_i^0)/L_i$ with respect to L_i $(0.5 \le L_i \le 1)$ for $k_i = 1$ and various values of L_i^0. As seen from the figure, q_i has the constant value 1 for the case of zero unstressed length with $L_i^0 = 0$. If L_i^0 has a moderate value, then q_i can vary in a wide range; e.g., $0.2 \le q_i \le 0.6$ for $L_i^0 = 0.4$.

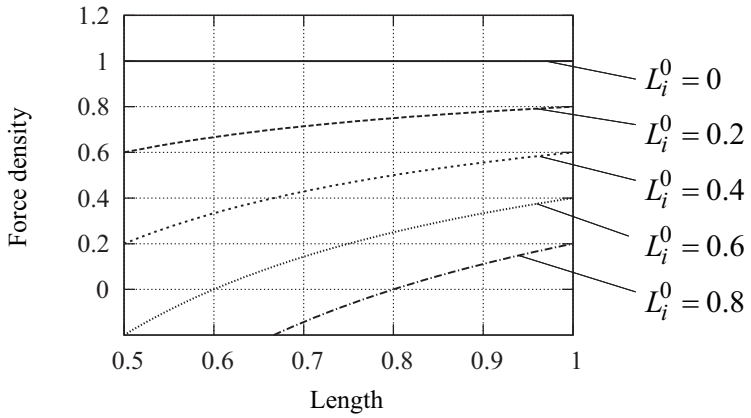

Fig 2. Variation of force density with respect to member length.

4.3 Summary of optimization process

The process of form-finding using optimization approach is summarized as follows:

Step 1. Assign material properties for cables and struts including fictitious material properties for some cables.

Step 2. Define a function of member lengths as an objective function to be minimized.

Step 3. Solve the optimization problem using any optimization algorithm.

Step 4. Assign the true material properties, and compute unstressed lengths so that the axial forces do not change from those determined in Step 3.

Step 5. Check stability of the self-equilibrium state using the true material properties.

In the numerical examples, optimization is carried out using SNOPT Ver.7 (Gill et al., 2002) that utilizes sequential quadratic programming (SQP). The sensitivity coefficients are computed analytically, e.g., as Eqs. (22) and (27) for $F(\mathbf{X}) = S(\mathbf{X})$. Let $\mathbf{H}^{(k)} \in \mathbb{R}^{3n\times 3n}$ denote the approximate Hessian of $F(\mathbf{X})$ at the *k*th step of SQP. The increment of $\mathbf{X}$ is denoted as $\mathbf{d} = \mathbf{X} - \mathbf{X}^{(k)} \in \mathbb{R}^{3n}$, which is the variable vector of the QP sub-problem at the *k*th step. Then, the sub-problem for the unconstrained problem is formulated as

$$\text{Minimize} \quad F^{(k+1)}(\mathbf{d}) = F(\mathbf{X}^{(k)}) + \nabla F(\mathbf{X}^{(k)})^T \mathbf{d} + \frac{1}{2}\mathbf{d}^T \mathbf{H}^{(k)} \mathbf{d} \tag{37}$$

When the approximate Hessian is singular at a step of SQP, a small diagonal term, which leads to a penalty term of the quadratic norm of the increment of variables, is added to $\mathbf{H}^{(k)}$. Therefore, for the analysis problem of a free-standing tensegrity structure, the rigid-body motions are automatically suppressed, and the nearest solution from the initial solution is obtained.

5. Constrained optimization and affine transformation for folding analysis

5.1 Constrained optimization for folding analysis

We consider a process of folding a tensegrity tower that consists of struts, vertical cables, saddle cables, diagonal cables, and horizontal cables (Zhang and Ohsaki, 2008; Micheletti and Williams, 2007; Sultan, 2014). The folding process is slow enough so that dynamic effect need not be considered, assuming existence of appropriate damping; therefore, we consider a quasistatic process of folding.

An example of three-layer tower is shown in Fig. 3. Folding analysis is carried out by assigning constraints on the difference between z-coordinate z_j^{U} of the j th node in the top ring and z-coordinate z_k^{L} of the k th node in the bottom ring as

$$z_j^{\mathrm{U}} - z_k^{\mathrm{L}} \le h, \quad (j = 1, \ldots, n^{\mathrm{R}};\ k = 1, \ldots, n^{\mathrm{R}}) \tag{38}$$

where n^{R} is the number of nodes in each ring, and h is the specified total height.

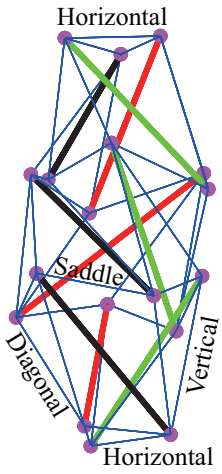

Figure 3. A 3-layer tensegrity tower model.

Folding is carried out by suppressing the top ring to the bottom. The parametric optimization problem for obtaining the equilibrium states in the folding process is formulated as

$$\begin{aligned} &\text{Minimize} \quad S(\mathbf{X}) = \sum_{i=1}^{m} S_i(L_i(\mathbf{X})) \\ &\text{Subject to} \quad z_j^{\mathrm{U}}(\mathbf{X}) - z_k^{\mathrm{L}}(\mathbf{X}) \le h, \quad (j = 1, \ldots, n^{\mathrm{R}};\ k = 1, \ldots, n^{\mathrm{R}}) \end{aligned} \tag{39}$$

where h is conceived as a parameter to be decreased from the initial value to 0.

Let λ_{jk} denote the Lagrange multiplier corresponding to the constraint $z_j^{\mathrm{U}} - z_k^{\mathrm{L}} \le h$. The reaction forces R_j^{U} and R_k^{L} for the j th node in the upper ring and the k th node in the lower ring, respectively, are computed from

$$R_j^{\mathrm{U}} = \sum_{k=1}^{n^{\mathrm{R}}} \lambda_{jk}, \quad R_k^{\mathrm{L}} = \sum_{j=1}^{n^{\mathrm{R}}} \lambda_{jk} \tag{40}$$

In the process of folding, cables should remain in tensile state. Therefore, it is desirable that the unstressed length of each cable is small enough compared with the length at equilibrium. However, as discussed in Sec. 2, it is very difficult to obtain an equilibrium

shape if unstressed cable lengths are too small. In this case, we can utilize affine transformation as shown below.

5.2 Folding of a tensegrity structure with zero-unstressed-length cables using affine transformation

Masic et al. (2005) proved that self-equilibrium equation of a tensegrity structure is invariant with respect to an affine transformation. This property can be easily observed using the equilibrium equations with respect to the nodal coordinates.

The self-equilibrium equation can be written using the force density matrix $\mathbf{Q}$ and the nodal coordinate vectors $\mathbf{x}$, $\mathbf{y}$, and $\mathbf{z}$ as Eq. (3). Obviously, these equations are satisfied with fixed $\mathbf{Q}$ and the coordinates after affine transformation as

$$\begin{aligned} \mathbf{x} &\to a_{11}\mathbf{x} + a_{12}\mathbf{y} + a_{13}\mathbf{z} + b_1\mathbf{I} \\ \mathbf{y} &\to a_{21}\mathbf{x} + a_{22}\mathbf{y} + a_{23}\mathbf{z} + b_2\mathbf{I} \\ \mathbf{z} &\to a_{31}\mathbf{x} + a_{32}\mathbf{y} + a_{33}\mathbf{z} + b_3\mathbf{I} \end{aligned} \tag{41}$$

where $\mathbf{I} \in \mathbb{R}^n$ is the vector that has 1 in all components. Using the affine transformation, various equilibrium shapes can be found after finding a single equilibrium shape.

Suppose we found an equilibrium shape using the zero-unstressed-length cables, and a forced deformation is applied to the structure. For a zero-unstressed-length cable, the axial force $N_i(\mathbf{X})$ is proportional to the length at equilibrium $L_i(\mathbf{X})$ as $N_i(\mathbf{X}) = k_i L_i(\mathbf{X})$, where k_i is the axial stiffness; i.e., k_i turns out to be the force density, as shown in Eq. (36), which does not depend on $L_i(\mathbf{X})$ in the process of forced deformation. Therefore, it is easily seen that the force density matrix does not change, and the structure can be deformed without external force, if there exists an affine transformation that does not change the strut lengths so that the force densities of all members are unchanged. This property has been discussed based on the theory of structural rigidity by Schenk et al. (2007).

Consider, for example, a tensegrity structure that is axisymmetric with respect to *z*-axis, and suppose there is only one class of struts; i.e., a strut can be moved to any other strut through a rotation around *z*-axis. In this case, there always exists an affine transformation

$$\mathbf{x} \to d\mathbf{x}, \quad \mathbf{y} \to d\mathbf{y}, \quad \mathbf{z} \to c\mathbf{z} \tag{42}$$

that preserves the strut lengths by appropriately assigning the coefficients *c* and *d*. This way, folding process is simulated without carrying out form-finding analysis; i.e, it can be simulated by successively decreasing *c* to 0 and finding *d* in Eq. (42) that does not change strut lengths.

6. Examples of tensegrity tower

6.1 Form-finding of 20-layer tower using bilinear fictitious material

To demonstrate the effectiveness of using fictitious bilinear elastic materials, the optimization approach is applied to form-finding of a 20-layer tensegrity tower as shown in Fig. 4(a). The units are omitted, in the following, for simple presentation of the results. The tower has three struts in each layer, and the radius and height of each layer are 20.0 and 22.5, respectively, at the initial state for solving optimization problem for minimization of the total strain energy.

Let e_i denote the ratio of unstressed length to the initial length. The values of e_i for cables and struts are assumed to be 0.8 and 1.0, respectively; i.e., the unstressed length of a cable is 80% of the length in the initial shape in Fig. 4(a), while the unstressed length of a strut is the same as the length in the initial shape. The value of A_iE_i for struts is 100000. As we demonstrated in Fig. 2, the values of e_i for cables should be sufficiently small to obtain various stable equilibrium shapes without slackening of cables.

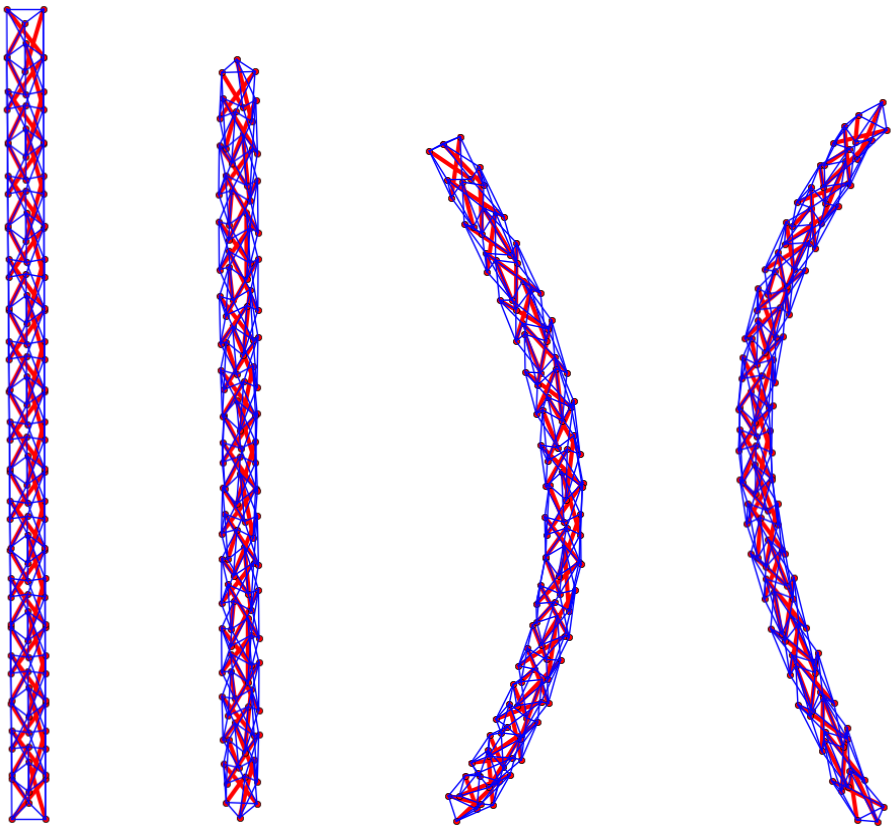

(a) (b) (c) (d)

Figure 4. Initial and self-equilibrium shapes of a 20-layer tensegrity tower; (a) initial shape, (b) equilibrium shape using a linear elastic material (Case 1), (c) equilibrium shape using a stiffening material (Case 2), (b) equilibrium shape using a softening material (Case 3).

Case 1:

We find the equilibrium shape using cables with linear elastic material denoted by Case 1 in Fig. 1, where $A_iE_i = 1000$, which is denoted by $A_iE_i^0$, for all cables. In this case, the stiffness of the true material is the same as that used in the form-finding process. The equilibrium shape obtained by solving the unconstrained optimization problem is shown in Fig. 4(b). The maximum axial force among all cables is 362.9. Eigenvalue analysis is carried out for the tangent stiffness matrix $\mathbf{K}_\mathrm{T}$ to find the 6th and 7th smallest eigenvalues as listed in the first row of Table 1. Since the 7th eigenvalue is sufficiently larger than the 6th eigenvalue that is approximately equal to 0, the equilibrium state is stable with six zero eigenvalues corresponding to rigid-body motions.

Table 1. Eigenvalues of tangent stiffness matrix using true material.

Case	6th	7th
1	6.140×10^{-6}	0.1303
2	1.520×10^{-7}	0.1253
3	4.540×10^{-7}	0.1107

Case 2:

We next consider a fictitious material with bilinear stress-strain relation. The 60 vertical cables are classified into six groups connecting the nodes with the same *xy*-coordinates in the horizontal plane of the initial shape in Fig. 4(a). Ten cables in one of the six groups are selected to have the stiffening bilinear stress-strain relation as indicated as Case 2 in Fig. 1. The strain $\hat{\varepsilon}$ at the stiffness transition point is 0.1, and the value of A_iE_i in the first and second parts are $A_iE_i^0\ (=1000)$ and $100A_iE_i^0\ (=100000)$, respectively. The equilibrium shape obtained by optimization is shown in Fig. 4(c). The minimum and maximum values of strains among the members with bilinear stress-strain relation are 0.1028 and 0.1030, which are close to $\hat{\varepsilon}\,(=0.1)$. This way, a curved shape can be generated by assigning large stiffness for the cables that are vertically aligned at the initial shape.

We compute the unstressed member lengths, and carry out eigenvalue analysis of the tangent stiffness matrix using the true material with constant value $A_iE_i = 1000$ for all cables. The 6th and 7th eigenvalues are listed in the second row of Table 1, which shows that the

structure is stable, although the true material has smaller stiffness than the fictitious material and the sufficient condition (30) for stability is not satisfied. If we set the maximum member length $L_i^{\mathrm{U}} = 1.1L_i^0$ in Eq. (31), which is consistent with $\hat{\varepsilon} = 0.1$, and solve the constrained optimization problem, almost the same equilibrium shape as shown in Fig. 4(c) is obtained. The axial forces and the Lagrange multipliers of the constrained members in layers 1, 3, and 5 are listed in Table 2. The axial forces obtained using the bilinear material are also listed in the first column of Table 2. It can be confirmed from these results that the cable forces at equilibrium can be obtained approximately as the sum of the differential coefficient $\partial S_i / \partial L_i$ and the Lagrange multiplier λ_i.

Table 2. Cable forces at equilibrium of constrained members in layers 1, 3, and 5.

Layer	Bilinear model	Constrained optimization		
		(A) Differential coefficient of strain energy	(B) Lagrange multiplier	(A) + (B)
1	397.6	100.0	300.1	400.1
3	380.2	100.0	282.6	382.6
5	380.8	100.0	283.2	383.2

Case 3:

Fictitious material property is given in the same vertical cables as Case 2, where $\hat{\varepsilon} = 0.1$ also for this case. We decrease the value of A_iE_i in the second part of the stress-strain relation of the ten vertical cables to $A_iE_i^0 / 100\,(=10)$ as indicated by Case 3 in Fig. 1. The equilibrium shape obtained by solving the unconstrained optimization problem is shown in Fig. 4(d). As seen from Figs. 4(c) and (d), the tower can be bent to opposite directions by increasing and decreasing the value of A_iE_i of the vertical cables in the specified group. The axial forces of the vertical cables with bilinear stress-strain relation are between 103.0 and 104.0, which are close to the specified value $0.1A_iE_i = 100$. We compute the unstressed member lengths, and carry out eigenvalue analysis of tangent stiffness matrix. The 6th and 7th lowest eigenvalues are listed in the third row in Table 1, which confirms the stability of structure. Since the stiffness of the fictitious material is smaller than that of the true material, the equilibrium shape with the true material is always stable, if the shape with fictitious material is stable.

6.2 Folding analysis of 2-layer tower

Folding analysis is carried out for a 2-layer tensegrity tower with three struts in each layer. Optimization problem is successively solved by varying the height h to be constrained in Eq. (38). The value of A_iE_i for the struts is 100000, which is sufficiently large, and a linear elastic material is used for cables. The unstressed lengths of cables should be sufficiently small to prevent slackening, while those of struts are the same as those in the initial shape.

We first consider the case $e_i = 0.2$; i.e., the unstressed length of each cable is 20% of the initial length. The value of A_iE_i for cables is 1000. The height of each layer of the initial shape is 40.0, i.e., the total height h is 80, whereas its radius r is taken as a parameter to solve the minimization problem of the total strain energy and obtain various self-equilibrium shapes. If r is small, the equilibrium shape approaches a straight line as shown in Fig. 5(a). If r is large, a planar shape is obtained as shown in Fig. 5(c).

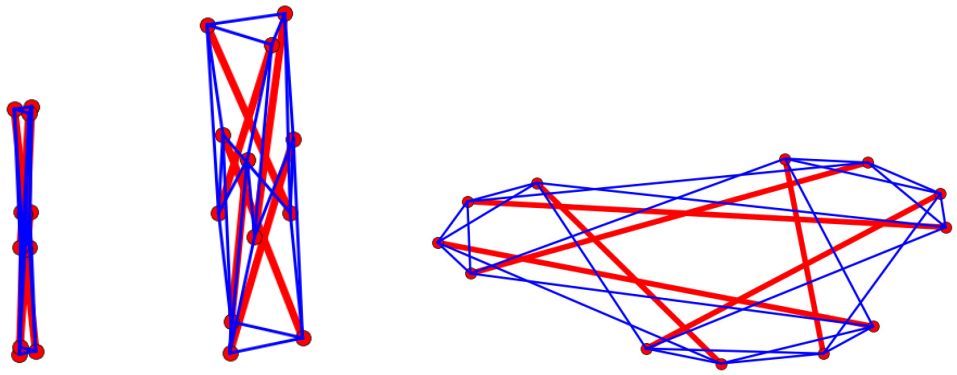

(a) (b) (c)

Figure 5. Equilibrium shapes for various initial radius for $e_i = 0.2$; (a) $r = 10$, (b) $r = 30$, (c) $r = 80$.

We assign $r = 30$ for folding analysis for various values of e_i. The equilibrium configuration without constrains is shown in Fig. 5(b), where the total height is 56.63. To prevent too large axial force at equilibrium, the value of A_iE_i is adjusted depending on the unstressed length of cable as

$$A_iE_i = 2000e_i \tag{43}$$

which leads to $A_iE_i = 1000$ for $e_i = 0.5$. It should be noted that the numerical results below depends on the value of A_iE_i.

The total reaction force at the top nodes during the folding analysis is plotted in Fig. 6 for each case of e_i with respect to the height h that is decreased to 0. For the range $e_i \geq 0.18$, the maximum reaction force increases as the unstressed length becomes smaller, and accordingly, the initial strain becomes larger. No reaction force exists at $h = 50$ for $e_i \leq 0.16$, because the height of equilibrium shape is less than 50 without constraint (38) on the height. The reaction forces are small for e_i = 0.12 and 0.1, and the equilibrium shape degenerates into a plane as e_i approaches 0, which agrees with the fact that a tensegrity structure with zero-unstressed-length cables cannot be obtained by energy minimization.

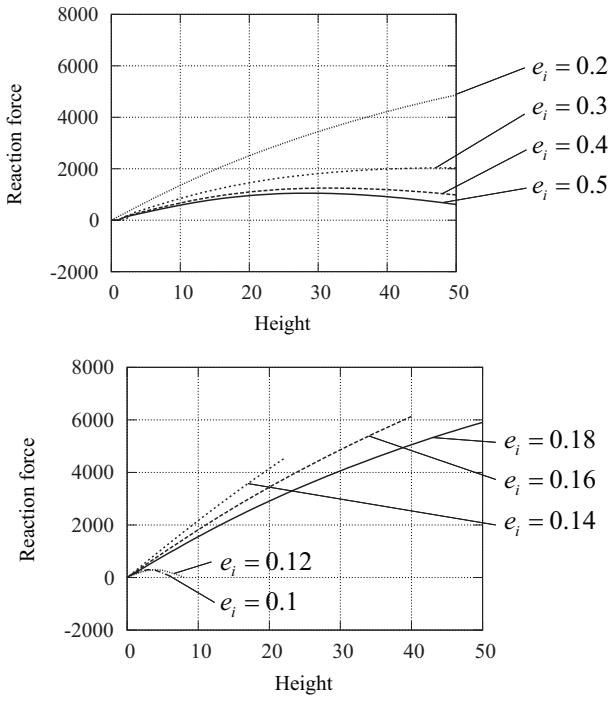

(a) (b)

Figure 6. Variation of reaction forces with respect to the specified height;
(a) e_i = 0.5, 0.4, 0.3, 0.2, (b) e_i = 0.18, 0.16, 0.14, 0.12, 0.1.

The force densities of struts are plotted with respect to the height in Fig. 7. The force densities for the cases $e_i \geq 0.18$ are normalized by the values at $h = 50$, whereas those for the cases are normalized by the value at the maximum height with non-zero reaction force. We

can see from Fig. 7(a) that the normalized force densities are close to 1, and are between 1 and 1.022 even for $e_i = 0.5$; therefore, the variation force density in the folding process is very small. Since a shape variation with constant force density matrix corresponds to an affine transformation, it is expected that the folding process can be approximately simulated using affine transformation without sucessively solving the constrained optimization problem.

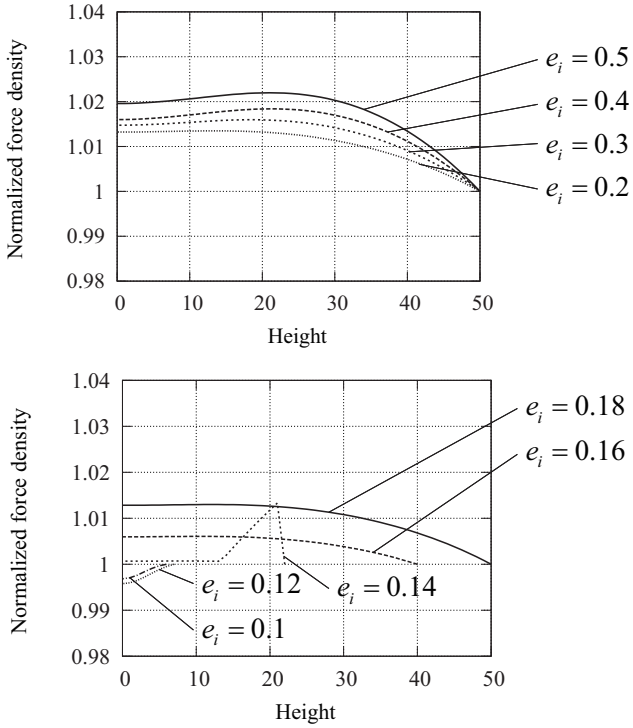

Figure 7. Variation of normalized force density of struts;
(a) $e_i = 0.5, 0.4, 0.3, 0.2$, (b) $e_i = 0.18, 0.16, 0.14, 0.12, 0.1$.

Although the value of e_i should be close to 0 to simulate the behavior of zero-unstressed-cable, we use $e_i = 0.1$ to prevent numerical difficulty in the optimization process. Furthermore, the initial radius r should be very large to prevent convergence to a thin shape as Fig. 7(a) when e_i has a small value; thus we set $r = 100$. The total height of the initial equilibrium shape without constraint is $h_0 = 133.9$, which is larger than the initial height 80, because the height becomes larger due to shrinkage of cables. Let c denote the ratio of the total height h to h_0. The radii of the circles, where the top/bottom nodes and middle nodes are located, at the equilibrium state are denoted by r_1 and r_2, respectively. Affine transformation in Eq. (42) is carried out to find the horizontal scale d so that the lengths of struts do not

change. The values of R_1, R_2, and the horizontal scale d are listed with respect to the height ratio c in Table 3.

Table 3. Variations of horizontal scale d, radii r_1 and r_2, and 7th and 8th eigenvalues of tangent stiffness matrix with respect to height ratio c of a tensegrity structure with zero-unstressed-length cables.

c	d	r_1	r_2	λ_7	λ_8	r_1^*	r_2^*
1.0	1.0	65.84	70.42	0.0107	2014.8	65.84	70.42
0.95	1.023	67.35	72.04	0.0110	2201.1	67.20	72.04
0.9	1.044	68.74	73.52	0.0111	2391.9	68.47	73.56
0.8	1.082	71.24	76.19	0.0112	2778.9	70.73	76.31
0.7	1.114	73.35	78.45	0.0120	2760.9	72.66	78.71
0.5	1.164	76.64	81.97	0.0090	1980.1	75.62	82.84
0.3	1.196	78.74	84.22	0.0050	1014.6	77.51	85.18
0.0	1.213	79.86	85.42	0.0	0.0	78.52	86.77

We can see from Table 3 that the horizontal scale and radii increase as the height is decreased. The values of radii obtained by solving constrained optimization problem (39) with $e_i = 0.1$ are listed as R_1^* and R_2^* in Table 3. Note that these values are slightly different from R_1 and R_2, because $e_i = 0.1$ indicates that the unstressed cable lengths do not vanish completely.

It has been confirmed that each configuration obtained using affine transformation has the self-equilibrium forces that are almost the same as the forces at equilibrium obtained by optimization with $e_i = 0.1$. According to Eq. (34), the axial stiffness k_i of zero-unstressed-length cable is equal to the force density. Since the equilibrium shape does not change when the stiffnesses of all members are scaled proportionally, we multiply 1.0×10^7 to the force density of each cable to obtain its stiffness. A large value 1.0×10^{10} is multiplied to the absolute value of the force densities of struts so that they can be assumed to be rigid compared with cables. The 7th and 8th eigenvalues λ_7 and λ_8 of the tangent stiffness matrix are listed in Table 3. It has been confirmed that the six lowest eigenvalues can be regarded as 0. Therfore, this result indicates that the structure in the folding process is stable; however, a

flexible deformation exists in the direction of the 7th eigenmode. Stability can also be confirmed for the equilibrium shape obtained by optimization with $e_i = 0.1$, because the equilibrium shape is found by energy minimization, and the reaction forces at the top and bottom have small positive values (compressive forces); e.g., for $c = 0.5$, the reaction force is 836.7, while the forces of struts are 13136.

7. Conclusions

An optimization approach has been presented for form-finding and folding analysis of tensegrity structures using fictitious material properties. The following conclusions have been obtained from this study:

1. Stability of the equilibrium shape obtained by optimization can be ensured without resort to tangent stiffness matrices. The stability is always guaranteed from local convexity of the objective function, if the gradient of objective function corresponds to the restoring force of a structure with fictitious material properties. Furthermore, the self-equilibrium state using the true material property is stable if the fictitious material used for form-finding has smaller stiffness than the true material.
2. Various equilibrium shapes can be obtained using fictitious material properties with bilinear elastic stress-strain relations. A curved tensegrity tower can be generated by assigning stiffening/softening materials for a group of vertically aligned vertical cables. A softening material can be used for finding a self-equilibrium state with the specified cable forces. It has been confirmed that the optimization problem with stiffening bilinear stress-strain relation is equivalent to a constrained optimization problem with upper bound for the member lengths.
3. When the unstressed cable lengths are reduced to zero, the axial force is assumed to be proportional to the length at equilibrium, and the axial stiffness should be proportional to the force density. In this case, there is generally no set of force densities that satisfies the rank defficiency condition of a tensegrity structure in 3-dimensional space; therefore, the equilibrium shape degenerates to a space of lower dimension; i.e., plane, line, or point. This property can be easily explained through similarity between form-finding problem of zero-unstressed-length cables and the problem of minimum square-length network.
4. Quasi-static folding of a tensegrity structure can be simulated by solving constrained optimization problems successively reducing the total height of the structure to be

specified. The reaction forces, which are computed from the Lagrange multipliers for the height constraints, first increases and then decreas as the height is reduced to 0. The force densities of members are almost constant for cables with small unstressed length compared with the length at equilibrium; however, the convergence property of optimization deteriorates when the unstressed cable lengths are very small.

5. Invariance of the equilibrium equations with respect to affine transformation can be simply explained using the invariance of force density matrix. Folding process of a structure with small unstressed-length cables can be approximately simulated using affine transformation.
6. The rigid-body motions need not be constrained when solving the optimization problem using an SQP method, because the quadratic programming sub-problem is automatically stabilized by assigning small positive values in the diagonals of the approximate Hessian of the Larangian.

Acknowledgements

The authors appreciste preliminary numerical investigation by Mr. Naoto Fujita (former graduate student of Hiroshima University) and Mr. Tetsuo Taguchi (graduate student of Hiroshima University).

References

Ali, N.B.H, Rhode-Barbarigos, L., Smith, I.F.C., 2011. Analysis of clustered tensegrity structures using a modified dynamic relaxation algorithm. Int. J. Solids Struct. 48, 637–647.

Arsenault, M., Gosselin C., 2005. Kinematic, static, and dynamic analysis of a planar one-degree-of-freedom tensegrity mechanism. J. Mech. Design, ASME 127, 1152–1160.

Arsenault, M., Gosselin C., 2005. Kinematic, static, and dynamic analysis of a spatial three-degree-of-freedom tensegrity mechanism. J. Mech. Design, ASME 128, 1061–1069.

Burkhardt, R., 2006. The application of nonlinear programming to the design and validation of tensegrity structures with special attention to skew prisms. J. Int. Assoc. Shell and Spatial Struct. 47(1), 3–15.

Chen, Y., Feng, J., Wu, Y., 2012. Novel form-finding of tensegrity structures using ant colony systems. J. Mech. Robotics, ASME 4, No. 031001.

Deng, H., Kwan, A.S.K., 2005. Unified classification of stability of pin-jointed bar assemblies. Int. J. Solids Struct. 42, 4395–4413.

Ehara, S., Kanno, Y., 2010. Topology design of tensegrity structures via mixed integer programming. Int. J. Solids Struct. 47, 571–579.

Gasparini, D., Klinka, K.K., Arcaro, V.F., 2011. A finite element for form-finding and static analysis of tensegrity structures. J. Mech. Materials Struct. 6, 1239–1253.

Gill, P.E., Murray, W., Saunders, M.A., 2002. SNOPT: An SQP algorithm for large-scale constrained optimization. SIAM J. Optim. 12, 979–1006.

Gueat, S., 2006. The stiffness of prestressed frameworks: A unifying approach. Int. J. Solids Struct. 43, 842–854.

Hanaor, A., 2012. Debunking "tensegrity": A personal perspective. Int. J. Space Struct. 27(2–3), 179–183.

Kanno, Y., Ohsaki, M., Ito, J., 2002. Large-deformation and friction analysis of non-linear elastic cable networks by second-order cone programming, Int. J. Numer. Meth. Engng. 55, 1079–1114.

La Salle, J., Lefscetz, S., 1961. Stability by Liapunov's Direct Method, Academic Press.

Li, Y., Feng, X.-Q., Cao, Y.-P., Gao, H., 2010. A Monte Carlo form-finding method for large scale regular and irregular tensegrity structures. Int. J. Solids Struct. 47, 1888–1898.

Masic, M., Skelton, R.E., Gill, P.E. 2005. Algebraic tensegrity form-finding. Int. J. Solids Struct. 42, 4833–4858.

Micheletti, A., Williams, W.O., 2007. A marching procedure for form-finding for tensegrity structures. J. Mech. Material Struct. 2(5), 857–879.

Miki, M., Mitani, J., Igarashi, T., 2013. Development of a Grasshopper add-on for interactive exploration of shapes in equilibrium. Proc. IASS Symposium 2013, Wroclaw, Poland, Int. Assoc. Shell and Spatial Struct.

Miki, M., Kawaguchi, K., 2010. Extended force density method for form-finding of tension structures. J. Int. Assoc. Shell and Spatial Struct. 51, 291–303.

Motro, R., 2003. Tensegrity: Structural Systems for the Future, Kogan Page Science.

Ohsaki, M., 2003. Optimum design of flexible structures under constraints on strain energy and asymptotic stability, Comp. Meth. Appl. Mech. Engng., Vol. 192, pp. 4487–4496.

Ohsaki, M., Nishiwaki, S., 2005. Shape design of pin-jointed multistable compliant mechanism using snapthrough behavior, Struct. Multidisc. Optim., Vol. 30, pp. 327–334.

Ohsaki, M., Tsuda, S., Watanabe, H., 2013. Optimization of retractable structures utilizing bistable compliant mechanism, Eng. Struct. 56, 910–918.

Ohsaki, M., Zhang, J.Y., 2006. Stability conditions of prestressed pin-jointed structures. Int. J. Non-Linear Mech. 41, 1109–1117.

Ohsaki, M., Zhang, J.Y., Elishakoff, I., 2012. Multiobjective hybrid optimization-antioptimization for force design of tensegrity structures. J. Appl. Mech. 79 (2), 021015-1-8.

Ohsaki, M., Zhang, J.Y., Kimura, S., 2005. An optimization approach to design of geometry and forces of tensegrities. Proc. IASS Symposium 2005, Bucharest, Int. Assoc. Shell and Spatial Struct., 603–610.

Pagitz, M., Tur, J.M.M., 2009. Finite element based form-finding algorithm for tensegrity structures. Int. J. Solids Struct. 46, 3235–3240.

Rhode-Barbarios, L., Schulin, C., Ali, N.B.H., Motro, R., Smith, F.C., 2012. Mechanism-based approach for the deployment of a tensegrity-ring module. J. Struct. Eng., ASCE. 138(4), 539–548.

Schenk, M., Guest, S.D., Herder, J.L., 2007. Zero stiffness tensegrity structures. Int. J. Solids Struct. 44, 6569–6583.

Skelton, R.E., de Oliveira, M.C., 2009. Tensegrity Systems, Springer.

Smaili, A., Motro R., 2005. A self-stress maintaining folding tensegrity system by finite mechanism activation. J. Int. Assoc. Shell and Spatial Struct. 45(3), 85–93.

Smaili, A., Motro R., 2007. Foldable/unfoldable curved tensegrity systems by finite mechanism activation. J. Int. Assoc. Shell and Spatial Struct. 47(3), 153–160.

Sultan C., 2014. Tensegrity deployment using infinitesimal mechanisms. Int. J. Solids Struct. 51, 3652–3668.

Sultan C., Skelton, R., 2003. Deployment of tensegrity structures. Int. J. Solids Struct. 40, 4637–4657.

Tibert, A.G., Pellegrino, S., 2003. Review of form-finding methods for tensegrity structures. Int. J. Space Struct. 18(4), 209–223.

Zhang L.-Y., Li Y., Cao Y.-P., Feng X.-Q., 2014. Stiffness matrix based form-finding method of tensegrity structures. Eng. Struct., 58, 36–48.

Zhang, J.Y., Ohsaki, M., 2006. Adaptive force density method for form-finding problem of tensegrity structures. Int. J. Solids Struct. 43, 5658–5673.

Zhang, J.Y., Ohsaki, M., 2007a. Stability conditions for tensegrity structures. Int. J. Solids Struct. 44, 3875–3886.

Zhang, J.Y., Ohsaki, M., 2007b. Optimization methods for force and shape design of tensegrity structures. Proc. 7th World Congress Struct. Multidisc. Optimiz. (WCSMO7), Seoul, 40–49.

Zhang, J.Y., Ohsaki, M., 2008. Numerical form-finding method for tensegrity tower. Proc.

IASS Symposium 2008, Int. Assoc. Shell and Spatial Struct., Acapulco, Mexico.

Zhang, J.Y., Ohsaki, M., 2013. Free-form design of tensegrity structures by non-rigid-body motion analysis, Proc. IASS Symposium 2013, Wroclaw, Poland, Int. Assoc. Shell and Spatial Struct., Paper No. 1306.

Zhang, J.Y., Ohsaki, M., 2015. Tensegrity Structures: Form, Stability, and Symmetry, Mathematics for Industry Series, Springer.